

Low-Loaded Pd–Pb/α-Al₂O₃ Catalysts: Indication of Alloy Formation from FTIR and X-Ray Photoelectron Spectroscopy

J. Goetz,* M. A. Volpe,† A. M. Sica,† C. E. Gigola,† and R. Touroude*,†

*Laboratoire d'Etudes de la Réactivité Catalytique, des Surfaces et Interfaces, URA 1498 du CNRS, 4 rue B. Pascal, F-67070 Strasbourg Cedex, France;
and †Planta Piloto de Ingeniería Química (UNS-Conicet), 12 de Octubre 1842, 8000 Bahía Blanca, Argentina

Received September 1, 1995; revised June 10, 1996; accepted December 6, 1996

Bimetallic Pd–Pb/α-Al₂O₃ catalysts with low metal concentrations have been characterized by Fourier transform infrared spectroscopy, H₂ chemisorption, and X-ray photoelectron spectroscopy (XPS). The samples have been prepared by reaction of tetra-*n*-butyl lead with prerduced monometallic Pd catalysts. The characterization of the base Pd/α-Al₂O₃ has been described in a previous paper (J. Goetz *et al.*, *J. Catal.* 153, 86 (1995)); it was found that particles having a large interaction with the support are formed when the Pd content is low. The addition of lead to monometallic Pd catalysts results in a decrease of hydrogen adsorption and important differences in IR spectra. Modification of XPS core level and Auger transitions of Pd were also observed, all results proving the formation of a Pd–Pb alloy. Analysis of Pb XPS spectra indicates that lead is present in two forms, namely Pb forming an alloy with Pd and Pb oxide located in the vicinity of Pd particles. Interaction between the metal particles and the support was not modified when adding Pb to the Pd particles. A model for the bimetallic particles is proposed where the penetration of Pb into the bulk of Pd is limited for particles having a large interaction with the support.

© 1997 Academic Press

INTRODUCTION

Palladium is the best known metal catalyst used for semi-hydrogenation of hydrocarbons with unsaturated carbon–carbon bonds (alkynes or dienes). Its remarkable intrinsic selectivity can, however, be improved by the addition of a second metal. Among the bimetallic catalysts, palladium–lead supported on calcium carbonate (Lindlar catalyst (1–3)) is widely used in organic syntheses, but its mode of action remains unexplained and the nature of the catalyst is not sufficiently understood. Controversy about the role of lead is reflected in several publications (4–6).

Pd–Pb/Al₂O₃ catalyst has been reported to show high selectivity in the hydrogenation of unsaturated hydrocarbons (7–10). However, in the literature dealing with these catalysts the oxidation state of the second metal, its localization

either on the support or on palladium particles and the possibility of alloy formation have not been analyzed. In the present study these different aspects have been explored in a series of Pd–Pb/α-Al₂O₃ catalysts by X-ray photoelectron spectroscopy (XPS), H₂ and CO chemisorption, and Fourier transform infrared spectroscopy (FTIR). The aim of this work is to characterize the Pd–Pb/α-Al₂O₃ catalysts in order to determine the role of lead in the improvement of the selectivity to semi-hydrogenation of unsaturated hydrocarbons.

The samples were prepared with different Pd and Pb contents, but in all of them the quantity of Pd metal was less than 0.30% in weight, in order to resemble the industrial catalysts. In a previous paper (11) we have studied the base monometallic catalyst, Pd/α-Al₂O₃, prepared from bis-acetylacetone of palladium. A characterization by transmission electron microscopy (TEM), XPS, and chemisorption was made and it was established that the electronic and physico-chemical characteristics of any given sample are intimately related to its Pd content, and more precisely to the concentration of the Pd complex solution used for the preparation. Two types of particles are formed, noninteractive and interactive, using solutions with high and low concentration of Pd complex, respectively.

The bimetallic catalyst preparation procedure is likely to control the type of palladium–lead interaction. Different methods exist for preparing bimetallic samples. We introduced lead to prerduced monometallic catalysts as an organometallic Pb compound in a liquid phase. In this way, according to previous studies (12, 13), a selective palladium–lead interaction is achieved and deposition of the second metal on the carrier is negligible.

EXPERIMENTAL

Catalyst Preparation

The preparation of the base monometallic catalysts has already been described (11). Tetra-*n*-butyl lead (Ventron, purity of 98.89%) was dissolved in *n*-heptane (Fluka, purity of 98.89%) at different concentrations, depending

¹ To whom correspondence should be addressed. Fax: (33) 88 41 61 47.
E-mail: touroude@chimie.u-strasbg.fr.

TABLE 1

Chemisorption Data for Pd-Pb/ α -Al₂O₃ Catalysts and their Monometallic Precursors

Pd-Pb (%)	H/Pd _{irr} (CO/Pd _{irr})	
	After 573 K reduction	After 773 K reduction
0.09	0.54 ^a	0.25 ^b
0.09-0.05	0.19 ^a	0.04 ^a
0.20	0.52 ^c	0.14
0.20-0.07	—	—
0.20-0.27	0.07	0.04 (0.02)
0.30	0.26 ^c (0.23)	0.23
0.30-0.05	0.10	0.12 (0.11)
0.30-0.12	0.10 (0.14)	0.04 (0.12)

^a Data taken from Ref. (8).^b Calculated from TEM value given in Ref. (11).^c Data taken from Ref. (11).

on the desired content. These solutions were put in contact at 298 K with prereduced monometallic catalysts. After approximately 3 h the solid was filtered and washed with *n*-heptane in order to eliminate the weakly adsorbed lead. The samples were then reduced under H₂ flow at 573 or 773 K for 1 h.

Table 1 gives the Pd and Pb weight concentrations determined by atomic absorption spectroscopy (AAS) for all samples. The nominal atomic ratios were determined from these values. The sample with 0.99-0.05% Pd-Pb was dominated by Aduriz *et al.* (8).

In order to investigate the possibility of lead deposition on the α -Al₂O₃, the same preparation procedure was followed for a support sample. The AAS analysis indicated that no lead had been fixed by the α -Al₂O₃.

H₂ and CO Chemisorption

Sorption and backsorption isotherms for H₂ or CO were measured on a standard glass volumetric apparatus. Prior to these measurements the samples were dried in He at 323 K, treated in H₂ at 573 K for 1 h, and evacuated overnight at the same temperature. The first isotherm, measured at room temperature, gave the total amount of adsorbed and absorbed gas. Subsequently, the samples were evacuated for 0.5 h and a second isotherm was obtained to determine the amount of adsorbed and weakly adsorbed gas removed during the evacuation step. The H/Pd or CO/Pd ratios were obtained by subtracting the second isotherm from the first. Hydrogen isotherms were measured in the 0- to 100-Torr pressure range. For CO, equilibrium pressures were selected in the 0- to 0.6-Torr range.

FTIR Spectroscopy

Infrared spectra of adsorbed CO were recorded using Nicolet 20 DXB spectrometer. The experiments were per-

formed in a stainless steel cell with CaF₂ windows mounted on Con-Flat flanges, coupled to a high vacuum system. Catalyst samples of about 30 mg were pressed to form transparent disks of 10 mm diameter and placed in the cell holder for pretreatment in H₂ at 573 K, cooling in He and evacuation. After recording a background spectrum, small amounts of CO were dosed using a leak valve up to a saturation pressure of 0.6 Torr. All IR spectra were recorded in the presence of this low gas phase pressure.

XPS Characterization of the Catalysts

The XPS experiments were performed using a VG ESCA III instrument equipped with an AlK α (1486.6 eV) anode. Spectra were taken after *in situ* reduction of the catalysts at 573 and 773 K. Reduction was carried out in the prechamber of the spectrometer at 1 atm (1 atm = 1.013 \times 10⁵ Pa) of high purity hydrogen for 1 h. After this treatment the samples were cooled to room temperature. Afterward the prechamber pressure was evacuated to 10⁻⁹ Torr (1 Torr = 133.3 Pa) and the samples were placed in the analysis chamber. The pressure in the spectrometer was lower than 10⁻⁸ Torr while collecting data.

O 1s, C 1s, Al 2s, Pd 3d, Ca 2p, Pb 4f X-ray photoelectron spectra and Pd MVV Auger spectra were obtained. When the elements were present at very low concentration, as was the case for Pd and Pb, 20 scans were accumulated in order to increase the signal to noise ratio. The scanning rate was 0.1 eV/s and the pass energy 20 eV. The Pb peaks were obtained by subtracting the 114- to 167-eV region of the bimetallic system from the equivalent range of the monometallic sample in order to eliminate the Al 2s plasmons.

An electrical charge effect shifts the XPS peaks by 2 or 3 eV toward higher binding energies (BE). The Al 2s peak (119.6 eV) was taken as a reference to correct the values, as explained elsewhere (11).

Theoretical curves were adjusted to fit the peaks by means of a home-made computer program. This procedure has been applied to the raw data points. A Doniach-Sunjic Lorentzian asymmetric function (14) was convoluted with an experimental Gaussian curve (*G*) which takes into account X-ray source broadening (AlK α _{1,2,3,4}), instrumental resolution, phonon excitation charging effects, and other possible sources of inhomogeneous broadening; this *G* value was extracted from the fitting of the Al 2s peak (119.6 eV) recorded when scanning 20 times the 114- to 167-eV region. A Shirley background (15) was subtracted. Values of BE, γ (half-width at half-maximum on the low energy side), and α (asymmetry index) were obtained. In the Doniach-Sunjic Lorentzian asymmetric function the parameter γ is directly associated with the natural linewidth of the hole state, inversely proportional to its lifetime, and α is related to the density of states (DOS) at the Fermi

level. As γ fits the broadening on the low BE side, it is not sensitive to the degree of asymmetry.

Relative metal intensities were calculated from peak surface ratio measurements after the Shirley background subtraction, corrected by difference in escape depths (a root square approximation was used) and difference in cross section (using Scofield's data (16)).

Due to the presence of Ca as an impurity in the alumina support, it was necessary to take into account Ca 2p lines and their satellites (due to $AlK\alpha_2, \alpha_3$ X-ray excitation source) which overlap the Pd 3d; afterward the deconvolution procedure was applied in order to eliminate the influence of Ca on the area and line shape. Spectra in the 325 to 365-eV range (fitting region) are illustrated in our previous paper (11).

The XPS analyses were repeated at least twice for each sample using two different pellets. The results were quite reproducible, both for the binding energy values and for the line shapes. The error in BE measurements was ± 0.1 eV whatever the catalyst.

Pd foil on which Pb was further deposited by evaporation was analyzed by XPS for use as reference samples. In this case, the Fermi level was taken as the BE reference. The Pd foil was first cleaned by argon sputtering for carbon and oxygen decontamination.

RESULTS

H_2 and CO Chemisorption

Table 1 summarizes the H/Pd and CO/Pd values for several bimetallic catalysts, reduced at 573 and 773 K. The data for the monometallic precursor catalysts (11) are also presented.

It is observed that the addition of Pb produces a marked decrease in the H_2 uptake whatever the monometallic precursor.

It is important to state that the 0.27% Pb loading on the 0.20% Pd catalyst cannot be exceeded (17). Using the initial Pd dispersion the number of surface Pd atoms (Pd_s) can be calculated, the Pb/ Pd_s ratio is then 1.3. A similar value has been found (8) for the 0.09% Pd sample upon saturation with $(C_4H_9)_4Pb$. Despite this high Pb content value, the sample retains a residual capacity to adsorb H_2 .

Another interesting observation is that the same H/Pd value was found for the Pd (0.30%) sample upon addition of 0.05 or 0.12% Pb, reduced at 573 K. Moreover, it is remarkable that, for both catalysts, 0.09% Pd/ α -Al₂O₃ and 0.3% Pd/ α -Al₂O₃, which are differently dispersed catalysts, their chemisorption values decrease by the same percentage (66%) after Pb has been added. These results suggest that the metal surface on these samples shows the same proportion of Pd and Pb atoms whatever the content of lead and the initial chemisorption values of the monometallic catalysts.

Increasing the reduction temperature to 773 K seems to further reduce the H/Pd values on Pd-Pb (0.30–0.12%)/ α -Al₂O₃ but not for the Pd-Pb (0.30–0.05%)/ α -Al₂O₃. The experimental error of these measurements prevents a better analysis of the hydrogen chemisorption results. In fact, for the samples with low chemisorption, the difference between reversible and irreversible uptake is very low in relation to the total adsorbed plus absorbed hydrogen. In these cases the CO isotherms can give more reliable results. Looking at the CO/Pd chemisorption measurements no change is significant when increasing the reduction temperature.

FTIR Spectroscopy

In Fig. 1 the FTIR spectra of CO adsorbed on 0.20 and 0.30% Pd/ α -Al₂O₃ are compared with those of (0.20–0.27%) and (0.30–0.12%) Pd-Pb/ α -Al₂O₃ respectively. For the monometallic samples, adsorption of CO in the linear form gives a band at 2085–2080 cm⁻¹; in addition a broad and intense band between 2000 and

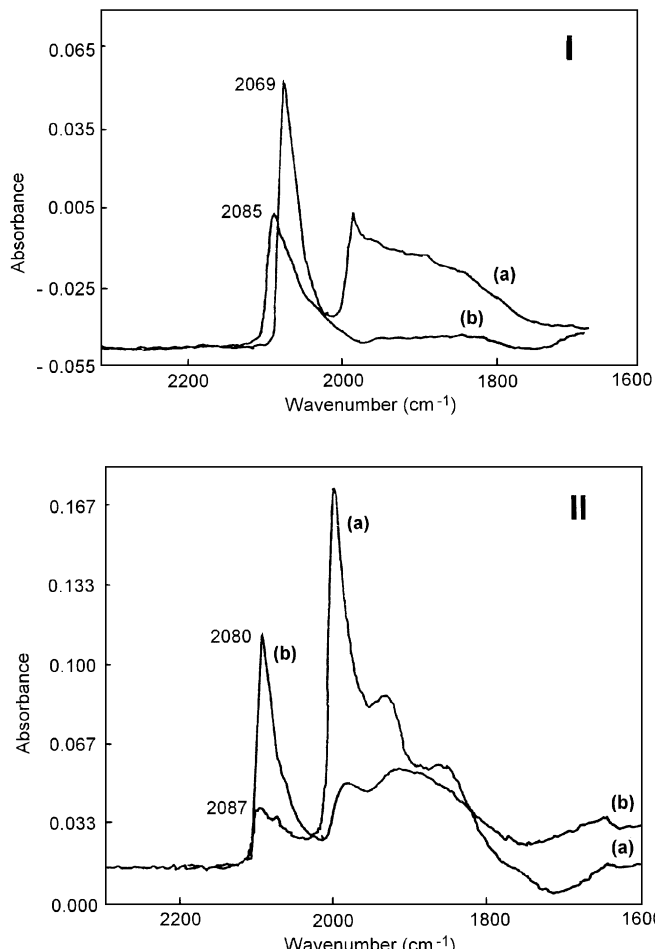


FIG. 1. FTIR spectra of adsorbed CO on Pd/ α -Al₂O₃ and Pd-Pb/ α -Al₂O₃ catalysts. (I) a, 0.20% Pd; b, 0.20% Pd-0.27% Pb. (II) a, 0.30% Pd; b, 0.30% Pd-0.12% Pb.

1700 cm⁻¹ that corresponds to CO bonded to two or three surface Pd atoms was observed. Upon Pb addition important changes were observed in the intensity of both the linear and bridged bands. The broad band at 2000–1700 cm⁻¹ was very small or almost absent while that of linear CO showed a large increase in intensity. The linear to bridged intensity ratio increased from 0.24 on 0.20% Pd/ α -Al₂O₃ to 3.4 on 0.20–0.27% Pd-Pb/ α -Al₂O₃ and from 0.14 on the 0.30% Pd/ α -Al₂O₃ to 0.49 on the (0.30–0.12%) Pd-Pb/ α -Al₂O₃. This behavior could be ascribed to the isolation of surface Pd atoms such that CO can only adsorb in the linear form. On the other hand, the decrease in frequency from 2085 to 2069 cm⁻¹ cannot be simply explained by a dilution effect, as the population of linear CO molecules in the bimetallic sample is larger.

XPS Pd Peaks

The 3d_{5/2} Pd BE values are reported in Table 2 for all the Pd-Pb/ α -Al₂O₃ series with the corresponding ones for the base monometallic samples (11). It must be remembered that the base monometallic catalysts presented characteristic shifts in 3d_{5/2} Pd BE when going from 0.30 to 0.20 and 0.09% Pd/ α -Al₂O₃ catalysts (0.5 and 1 eV shift respectively). It is clear that each bimetallic has kept the characteristic BE from its precursor. However, a slightly higher BE was found in the bimetallic catalysts compared with their corresponding base monometallic catalysts, even when the 0.1 eV error in BE measurement was taken into account. On the other hand, a narrowing effect in the width of the Pd 3d core level lines has been revealed in the bimetallic catalyst compared to the corresponding monometallic one. A series of examples is illustrated in Fig. 2 where the lines for bimetallic and base monometallic catalysts are reported after recalibration of both spectra to the same intensity and same BE in order to appreciate the narrowing effect more easily.

TABLE 2

Pd BE, α , and γ Parameters in Pd/ α -Al₂O₃ and Pd-Pb/ α -Al₂O₃ Catalysts Reduced at 573 and 773 K

Pd-Pb (wt%)	Pd 3d _{5/2} after reduction at 573 K			Pd 3d _{5/2} after reduction at 773 K		
	BE (eV)	γ	α	BE (eV)	γ	α
0.09	336.1	0.56	0.04	335.9	0.57	0.05
0.09–0.05	336.4	0.34	0.01	336.2	0.42	0.01
0.20	335.4	0.49	0.10	335.2	0.32	0.13
0.20–0.07	335.9	0.23	0.04	335.7	0.20	0.05
0.20–0.27	335.7	0.18	0.06	335.9	0.10	0.04
0.30	335.1	0.31	0.11	335.2	0.28	0.12
0.30–0.05	335.3	0.32	0.09	335.2	0.32	0.07
0.30–0.12	335.4	0.33	0.06	335.4	0.27	0.03

Note. The error in BE determination is ± 0.1 eV.

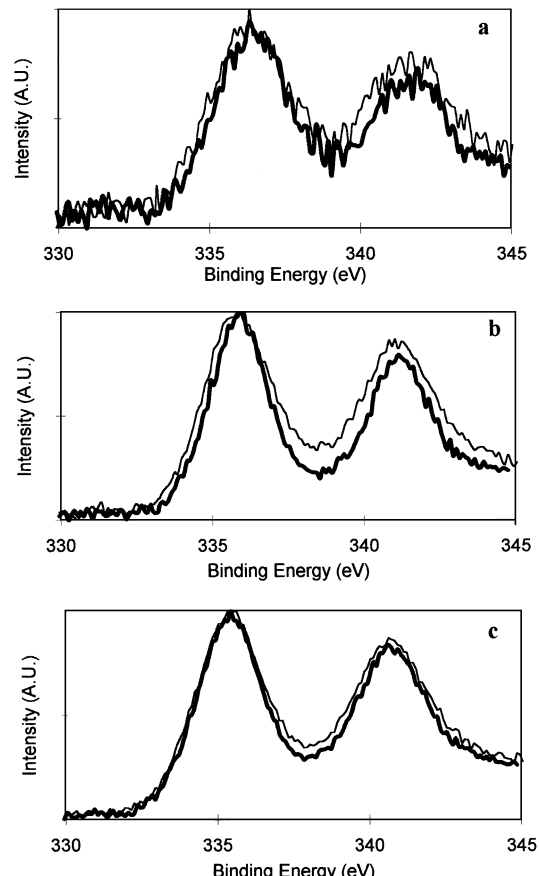


FIG. 2. XPS 3d region for Pd-Pb/ α -Al₂O₃ and the corresponding base Pd/ α -Al₂O₃, reduced at 573 K. (a) 0.30% Pd (—), 0.30% Pd-0.12% Pb (—); (b) 0.20% Pd (—), 0.20% Pd-0.27% Pb (—); (c) 0.09% Pd (—), 0.09% Pd-0.05% Pb (—).

We attempted to analyze quantitatively this narrowing phenomenon by fitting the curves as described under Experimental. We estimated that the signal to noise ratio (see Fig. 2) and the reproducibility was good enough to draw information from this procedure. Therefore γ (half-width at half-maximum on the lower energy side) and α (asymmetry index) values could be estimated. The results are reported in Table 2. The value of α tends to decrease when Pd-Pb/ α -Al₂O₃ catalysts are compared with the corresponding monometallic catalyst. In spite of the reduction treatment, γ remains almost constant when lead is added to the 0.30% Pd catalyst, but γ is smaller for the bimetallic catalysts than for the monometallic precursors in both the 0.20 and the 0.09% Pd samples.

It may be added that, when Pb was evaporated on the Pd foil at room temperature, no change in the Pd 3d line shape was observed.

Although the Pd MVV Auger lines are poorly resolved, it is possible to detect a slight modification in the line shape and a more defined doublet structure for the bimetallic catalysts, as is illustrated in Fig. 3. The same tendency was

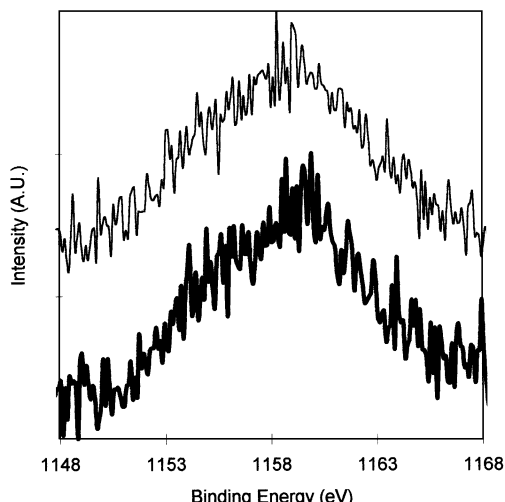


FIG. 3. Pd MVV Auger spectra for Pd-Pd/α-Al₂O₃ and the corresponding Pd/α-Al₂O₃ reduced at 573 K. 0.30% Pd-0.12% Pb (—), 0.30% Pd (—).

observed for Auger lines corresponding to all the other catalysts.

Finally in Table 3, (Pd/Al)_{XPS} ratios are reported for both mono- and bimetallic catalysts. It is seen that the ratios remain nearly constant when adding lead.

XPS Pb Peaks

Figure 4 shows the region corresponding to the Pb 4f_{7/2} and 4f_{5/2} doublet for three bimetallic samples. The dotted lines represent the raw spectra after subtracting Al 2s plasmons. Even though the signal to noise ratio is not so good for low lead content, it is visible that each peak in the doublet transition is not a unique one but is a summation of several contributions. Moreover, the contributions at higher binding energy decrease when the reduction temperature increases, so they can be assigned to lead oxide. An attempt was made to fit these peaks in order to appreciate roughly

TABLE 3
(Pd/Al)_{XPS} Ratios for Monometallic Pd and Bimetallic Pd-Pb Catalysts

Pd-Pb (%)	(Pd/Al) _{bulk} (10 ⁴)	(Pd/Al) _{XPS} (10 ³)	
		Reduced at 573 K	Reduced at 773 K
0.09	4.31	2.6	2.2
0.09-0.03		2.6	3.0
0.20	9.58	6.5	5.9
0.20-0.07		7.6	6.6
0.20-0.27		6.2	5.1
0.30	14.37	9.0	8.5
0.30-0.05		9.3	8.6
0.30-0.12		8.4	8.1

TABLE 4

Pb⁰ and Pb⁽⁺⁾ BE, Pb⁽⁺⁾ Percentages, and Difference between Pd 3d_{5/2} and Pb 4f_{7/2} BE for Pd-Pb/α-Al₂O₃ Catalysts Reduced at 573 and 773 K

Pd-Pb (%)		BE Pb ⁰ 4f _{7/2} (eV)	BE Pb ⁽⁺⁾ 4f _{7/2} (eV)	%Pb ⁽⁺⁾ (%)	Pd-Pb diff. ^a (eV)
0.09-0.05	a	137.5	139.0	59.1	198.5
	b	137.6	139.6	12.9	
0.20-0.07	a	137.2	139.1	32.5	198.4
	b	137.4	139.1	7.6	
0.20-0.27	a	137.1	139.5	28.8	198.5
	b	137.3	139.1	18.2	
0.30-0.05	a	136.4	138.0	35.0	198.6
	b	136.7	—	0	
0.30-0.12	a	137.0	139.1	47.2	198.0
	b	136.7	—	0	
Pb evaporated onto foil		137.0			198.2

Note. a, reduced at 573 K; b, reduced at 773 K.

^a Pd 3d_{5/2} BE in Pd/α-Al₂O₃-Pb 4f_{7/2} BE in Pd-Pb/α-Al₂O₃.

the content of oxidized lead (Fig. 4). As a first approximation, we considered only two lead contributions in the 4f_{7/2} peaks and their counterparts in 4f_{5/2} peaks. We shall call the lead related with the doublet at lower BE Pb⁰. In fitting these peaks we fixed the surface ratio between both transitions at the theoretical value of 1.33. γ was also kept constant at 0.40 eV. The BE values are given in Table 4, second column. We shall call the other contribution to the doublet transition Pb⁽⁺⁾. The corresponding BE, reported in the third column, was found to be 2 ± 0.5 eV higher than that of Pb⁰, except for the 0.30-0.05 sample reduced at 773 K where the BE could be considered erroneous because of the low Pb⁽⁺⁾ concentration.

The estimated percentage of Pb⁽⁺⁾ is also shown in Table 4. A decrease in this area value was observed when reducing at 773 K.

In the last row of Table 4, we have reported the difference between the Pd 3d_{5/2} BE of the precursor Pd/α-Al₂O₃ and the Pb⁰ 4f_{7/2} BE of the corresponding bimetallic catalyst.

The Pb/Pd atomic ratios are reported in Table 5. The nominal ratios are given in column 2 and the observed (Pb_{tot}/Pd)_{XPS} ratios in column 4. As lead oxide was quantified, it could be deduced from the total amount of lead and one calculates (Pb⁰/Pd)_{nominal} and (Pd⁰/Pd)_{XPS} as reported respectively in columns 3 and 5. The (Pb_{tot}/Pd)_{XPS} ratios do not change when the reduction temperature increases; on the contrary, the (Pb⁰/Pd)_{XPS} ratios increase with reduction temperature. This is not an indication of Pb segregation but occurs because nearly all the oxidized lead is reduced at high temperature. On catalysts reduced at 773 K in which the oxidized lead is minimized, the (Pb_{tot}/Pd)_{XPS} is equal to the (Pb/Pd)_{nominal} for catalysts in which the (Pb/Pd)_{nominal} is

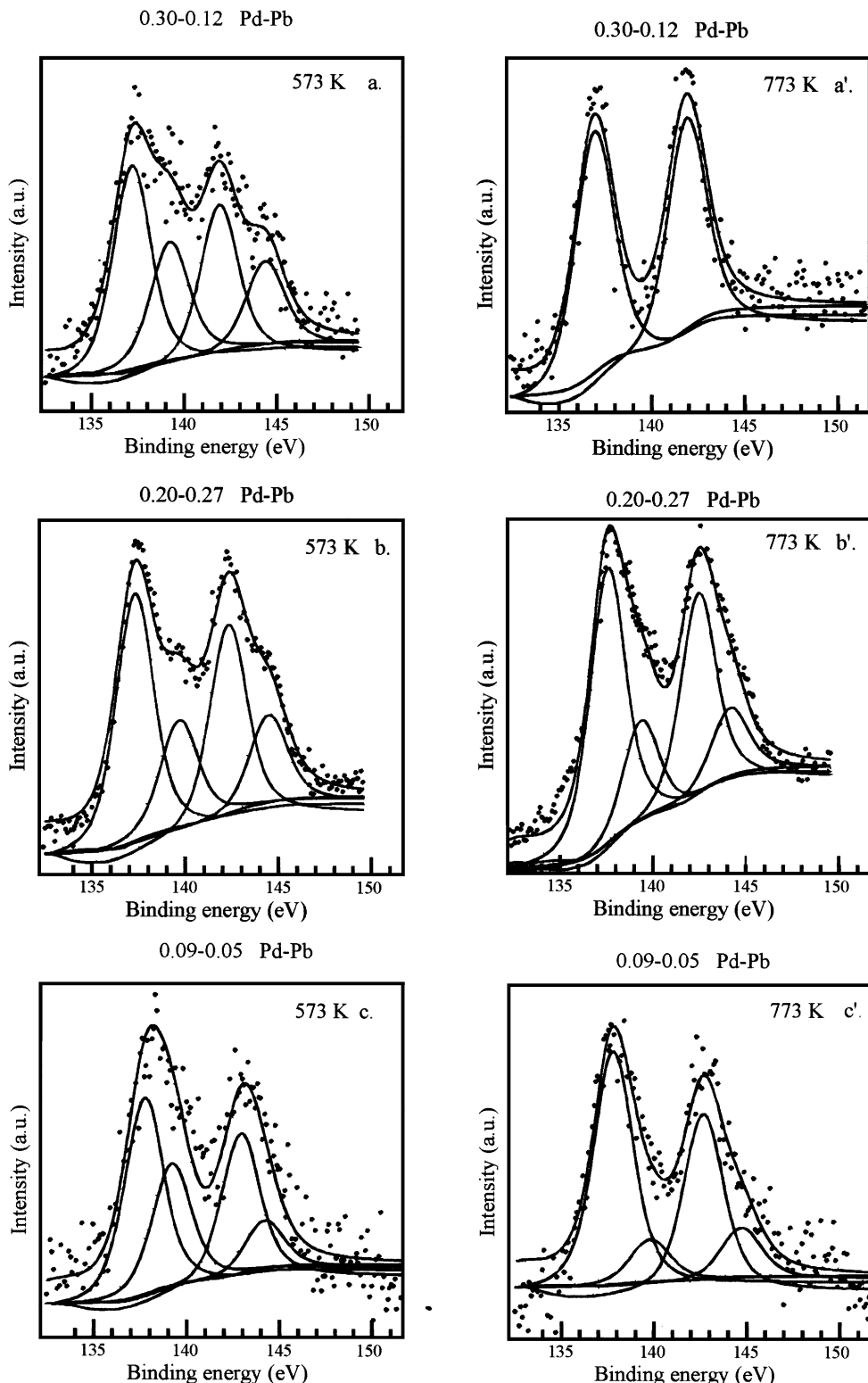


FIG. 4. XPS Pb 4f region for Pd-Pb/ α -Al₂O₃ reduced at (a), (b), (c) 573 K, and (a'), (b'), (c') 773 K. (a, a') 0.30% Pd-0.12% Pb, (b, b') 0.20% Pd-0.27% Pb, (c, c') 0.09% Pd-0.05% Pb.

TABLE 5
 $(\text{Pb}/\text{Pd})_{\text{XPS}}$ and $(\text{Pb}/\text{Pd})_{\text{nominal}}$ Atomic Intensity Ratios

Catalysts Pd-Pb (weight %)	$(\text{Pb}/\text{Pd})_{\text{nominal}}$	(Pb^0/Pd)	$(\text{Pb}_{\text{tot}}/\text{Pd})_{\text{XPS}}$	$(\text{Pb}^0/\text{Pd})_{\text{XPS}}$	$T(\text{K})$
0.09–0.05	0.29	0.12	0.44	0.18	573
		0.25	0.48	0.42	773
0.20–0.07	0.18	0.12	0.23	0.15	573
		0.17	0.22	0.20	773
0.20–0.27	0.69	0.49	0.8	0.57	573
		0.56	1.2	0.98	773
0.30–0.05	0.09	0.06	0.06	0.04	573
		0.09	0.09	0.09	773
0.30–0.12	0.21	0.11	0.18	0.10	573
		0.20	0.20	0.19	773

lower than 0.3. This is also seen in Fig. 5 where $(\text{Pb}/\text{Pd})_{\text{XPS}}$ ratios obtained at 773 K reduction temperature are reported as a function of $(\text{Pb}/\text{Pd})_{\text{nominal}}$ ratios. When the ratio is equal or higher than 0.3 the $(\text{Pb}/\text{Pd})_{\text{XPS}}$ values are higher than the nominal ones; in this latter case there is segregation of lead on the surface.

DISCUSSION

Chemisorption and FTIR Results

The interaction of Pb with surface Pd atoms produces a notable effect on the adsorption of H_2 and CO. The decrease in H_2 chemisorption and the large increase in the linear to bridge intensity ratio of adsorbed CO indicates that Pb suppresses the adsorption of species that require an ensemble of atoms. It was shown (18) that, on monometallic supported Pd catalysts, the linear CO is preferentially formed on low coordinated Pd atoms, on edges and cor-

ners, while bridged CO is adsorbed on high coordinated Pd atoms, that is, on surface planes. The depletion of bridged CO upon Pb addition means that Pb atoms are not located on the corners and on the edges as would be expected from a decoration model but they are mainly positioned on terraces and play the role of dilution of the Pd surface atoms.

If an alloy is formed, the possibility of a ligand effect of Pb on the chemisorption properties of Pd may be revealed by changes in the IR band frequencies. It is well known that the position of IR bands depends on the surface coverage, due to intermolecular interactions, and a shift to lower frequencies is usually observed as the coverage decreases. In a bimetallic catalyst a similar shift may be due to geometric or electronic factors. In our case if an alloy is formed, the replacement of Pd atoms by Pb increases the distance between the adsorbed CO molecules and the coupling of dipoles is reduced (geometric effect), leading to lower frequencies. However, our Pd-Pb samples also show a pronounced increase in intensity which indicates that the number of linear CO molecules is much higher than that on $\text{Pd}/\alpha\text{-Al}_2\text{O}_3$, and therefore an increase in dipole-dipole coupling, and an increase in frequency, should be expected. Consequently, the 16 cm^{-1} frequency downshift in the Pd-Pb (0.2–0.27%) sample may reflect the existence of both the ligand and the geometric effect. It is worth mentioning that a similar situation was found to be present in silica-supported Pd-Ag alloys (19) and in the Pt-Pb system (20) where the isotopic dilution method was used to separate the contribution of dipole-dipole coupling from an electronic interaction between the alloy components. In addition to a frequency downshift we have found that the linear CO absorption band is more stable on Pd-Pb: a 90% decrease in integrated intensity, after 2 min vacuum, was observed for the 0.2% Pd sample, while on Pd-Pb it was about 50%, indicating a stronger adsorption bond on the bimetallic catalyst.

In order to advance an interpretation that relates these observations, it is convenient to examine the bonding of CO with the metal surface in terms of some recent theoretical studies (21, 22). It is well known that the adsorption of CO on Pd takes place mainly in the bridging mode. According to Anderson and Awad (23), this is so because the energy level of the metal valence band is closer to the $2\pi^*$ level of CO which in turn enhances the back donation of metal d and s electrons to the empty antibonding orbital of CO. The high $2\pi^*$ population explains the infrared bands in the $2000\text{--}1700\text{ cm}^{-1}$ frequency range. Assuming that a Pd-Pb alloy is formed, the valence band narrows (27) and the effect of back donation is reduced. Consequently, the chemisorption of CO will shift to the linear form where σ bonding predominates and the characteristic IR frequency is determined only by interaction of $2\pi^*$ orbitals with metal d electrons. However, its value may be different from that of linear CO on pure Pd, due to the change in metal coordination. The weak linear adsorption of CO on $\text{Pd}/\alpha\text{-Al}_2\text{O}_3$ takes

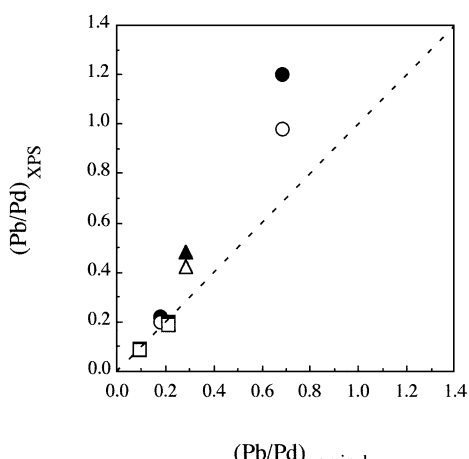


FIG. 5. $(\text{Pb}/\text{Pd})_{\text{XPS}}$ versus $(\text{Pb}/\text{Pd})_{\text{nominal}}$ for catalysts reduced at 773 K. ▲, $\text{Pb}_{\text{tot}}/\text{Pd}$ (0.09% Pd); △, Pb^0/Pd (0.09% Pd); ●, $\text{Pb}_{\text{tot}}/\text{Pd}$ (0.20% Pd); ○, Pb^0/Pd (0.20% Pd); ■, $\text{Pb}_{\text{tot}}/\text{Pd}$ (0.30% Pd); □, Pb^0/Pd (0.30% Pd).

place on metal atoms of low coordination (edge and corner atoms), at 2080–2085 cm⁻¹, while on Pd-Pb/ α -Al₂O₃ linear CO, at 2069 cm⁻¹, adsorbs indifferently on edge, corner, and face atoms, isolated from each other by Pb atoms. Therefore, on bimetallic catalysts, the main part of the linear CO band comes from CO adsorbed on face Pd atoms. These atoms possess a higher coordination number compared with the edge and corner Pd atom of the monometallic catalysts. This could explain the lower IR frequency and the stronger metal–carbon bond for the linear CO on bimetallic catalyst because, as discussed by Nieuwenhys *et al.* (24), the width of the d band increases with the coordination number, so a larger interaction with the antibonding orbital of CO takes place. We recognize some limitations to the above argument, because it is difficult to predict the changes in Pd coordination, and the corresponding alterations in the valence band due to the replacement of transition metal atoms by Pb. However, the FTIR results can be easily interpreted if one assumes the formation of a Pd–Pb alloy.

XPS Pd Peaks

Knowing the difficulty in extracting information from the XPS spectrum of supported catalysts due to the low content of metal, charge effects, and particle size distribution, we limited our analyses to the comparison of the bimetallic catalysts with their monometallic precursors, all the spectra being recorded and treated in the same manner. Moreover it should be underlined that the bimetallic catalysts were prepared by addition of tetrabutyl-lead to the monometallic precursor catalyst reduced at 573 K, followed by a decomposition under hydrogen at 573 and 773 K. This minimizes the changes in size and shape of Pd particles which could occur during the preparation process except those due to the interaction of Pb with Pd. Furthermore, except for the 0.2% Pd catalyst which has a complex structure (11), it should be noticed that the binding energy and the line shape (α , γ) do not change for the 0.09 or the 0.3% Pd catalyst when the reduction temperature increases from 573 to 773 K, while the particle size in the 0.09% Pd catalyst increases from 2.8 to 4.5 nm (TEM analysis 11). Therefore any modification of the Pd peaks after Pb addition to these catalysts can hardly be attributed to a change of Pd particle size.

The 0.2% Pd catalyst showed a clear bimodal distribution (TEM micrograph (11)) after reduction at 573 K. That could explain the intermediate values found in the XPS spectrum analysis for BE, α , and γ . In fact the XPS spectrum of the 0.2% Pd catalyst reduced at 573 K can be neatly fitted using two Pd contributions, one with the characteristics, BE, α , and γ of the 0.3% Pd catalyst and the other with those of the 0.09% Pd catalyst. In this way we estimated that the 0.2% Pd catalyst contains 60% of noninteractive particles (BE, 335.1 eV) and 40% of interactive particles (BE, 336.1 eV). This is not a proof of the bimodal distribu-

tion but correlates well with the TEM observation. When increasing the reduction temperature, the line shape of the Pd 3d spectrum shows a smaller γ , 0.31 instead of 0.56 (see Table 2); fitting the corresponding spectrum with two Pd contributions leads to an increase of the proportion of non-interactive particles to 90%. This is in agreement with the other characterization analysis which showed a monomodal particle size with 7.7 nm as the mean particle diameter for the catalyst reduced at 773 K. The addition of 0.27% Pb to the 0.2% Pd catalyst, possessing a bimodal particle size distribution when reduced at 573 K, has led to an important narrowing effect in the line shape of the Pd 3d line (Fig. 2, spectrum b) whatever the following H₂ treatment (573 or 773 K) and a noticeable higher binding energy. These peaks can fit only with one Pd contribution and reveal a large modification in the Pd particles due to Pb penetration inside the particles. In fact, taking into account the dispersion of the 0.2% Pd catalyst and the content of metallic Pb one may calculate that each surface Pd atom would have to accommodate approximately one Pb atom. Knowing that the Pb atomic volume is twice that of Pd and noting that this catalyst is still able to chemisorb H₂ and CO, it is obvious that Pb penetrates inside the particle.

In the presentation of the Pd XPS results (Table 2) we have seen that, whatever the reduction temperature, γ values for Pd-Pb/ α -Al₂O₃ catalysts are smaller than the corresponding ones for Pd/ α -Al₂O₃, except for the pair of 0.30% Pd samples. Otherwise, when comparing α values for the mono- and bimetallic catalysts, we can observe that the asymmetry of the Pd/ α -Al₂O₃ samples is always smaller for the bimetallic catalysts. For α , the physical interpretation is related to relaxation phenomena that take place after photoelectron ejection (25). The electrons at the Fermi level can be excited to higher unoccupied levels; in this way electron–hole pairs are created and these increase the peak asymmetry. A decrease of the asymmetric parameter is generally explained by a diminution in the density of states at the Fermi level. This density change is produced when alloying metals or when going from bulk to small metal particles. Our interpretation of the variation in the asymmetric parameter is based on the assumption of the existence of a strong interaction between Pd and Pb that gives rise to electronic modification of the valence band of Pd. These changes would decrease the number of electrons at Fermi level and thus reduce the asymmetry in the core level peak.

van Attekum *et al.* (26) have reported variations in the core level lineshapes of different alloys; an asymmetric narrowing was reported for PtBi, AgAu, and PdSb core levels. The authors reported 0.56 and 0.54 eV as nearly constant values of γ for Pd and PdSb, respectively, and found an important variation in the α parameter (0.20 and 0.02 eV for the Pd and PdSb, respectively). We, however, have not observed a constancy in γ for the low loaded samples (0.20 and 0.09% Pd). This discrepancy could be explained by

taking into account the fact that the above authors analyzed bulky unsupported alloys, which are approximately comparable with Pd particles in the sample with the highest metal content. On the contrary, in the other catalysts, the metal particles interact with the support (11) and that could lead to special features.

The valence band density of states information is linked with the lineshape of Auger peaks. We could detect a slight but definite peak lineshape modification in Pd MVV Auger lines when going from the mono- to the bimetallic system. An analysis of the valence band corresponding to a Pd cluster containing 43 atoms and a Pd₃Pb cluster with 31 Pd and 12 Pb atoms has been made in a theoretical approach (27) and a narrowing of the valence band and a Fermi level shift were found when going from the Pd cluster to the Pd₃Pb cluster.

In every Pb containing catalyst the Pd 3d_{5/2} peak lies at a slightly higher BE than in the Pd/α-Al₂O₃ series. A positive shift with respect to metallic Pd has been reported in intermetallic compounds (28, 29). According to previous XPS studies on Pt-Ge/Al₂O₃ and Pt-Sn/Al₂O₃ (30, 31), the Pt 4d_{5/2} peak is found at larger BE in the case of the bimetallic catalysts as compared to the monometallic sample; the respective authors attributed these shifts to Pt in the bimetallic sample being in a more electron-deficient state. Biloen *et al.* (32) have also reported a larger BE value for Pt in the Pt-Re/SiO₂ system as compared with the monometallic case and this was said to be an effect of Pt-Re alloy formation leading to an electronic modification of Pt. Due to the small shift observed in our study, that is not a definitive argument to support the formation of an alloy.

XPS Pb Peaks

Let us concentrate on the second column in Table 4 reporting Pb⁰ binding energies. These values are not constant. For samples reduced at 573 K, the shift in binding energy from one sample to another is nearly the same as that observed for the Pd BE in the respective precursor Pd/α-Al₂O₃; in other words, the difference between Pb⁰ 4f_{7/2} in bimetallic samples and Pd_{5/2} in the corresponding base monometallic catalyst is nearly constant (198.3 ± 0.3 eV). This value is the same as the one found when evaporating Pb on Pd foil (see the last row of Table 2). Therefore we could consider that Pb is in the metallic state and in electrical contact with Pd. The reason why the monometallic catalysts have different Pd BE values has already been discussed (11) and was correlated with different types of interaction between the metal particles and the support.

With regard to Pb⁽⁺⁾, it is difficult to assign a given species to this doublet. We cannot distinguish between all possible lead oxides for which we do not have our own references. Kim *et al.* (33), examined several lead oxides by XPS; they have reported 136.9 eV for Pb⁰ 4f_{7/2} and 137.9 and 137.5 eV

for PbO and PbO₂, respectively. In addition the spectrum of Pb₃O₄ was deconvoluted into two contributions, Pb²⁺ and Pb⁴⁺, at 138.9 and 137.9 eV, respectively. Taking into account their results, we could assign the Pb⁽⁺⁾ peak to Pb₃O₄, although, if some forms of lead are in strong interaction with alumina, their BE cannot be distinguished from that of lead oxide.

According to our results, the percentage of Pb⁽⁺⁾ decreases when the samples are reduced at 773 K. It is well known that lead oxides are hard to reduce; Wendt and Meinecke (34) found that a temperature as high as 900 K is necessary to reduce PbO on α-Al₂O₃. In our Pd-Pb/α-Al₂O₃ systems a partial reduction takes place without difficulty. To explain this phenomenon we can argue that Pb oxide is located on the support around the particles or on the alloy particles. We can therefore assert that there are no isolated lead oxide particles on the support. Moreover, as we found that the (Pd/Al)_{XPS} ratios do not change significantly when adding Pb to the monometallic precursor (see Table 3), Pb oxide could not be considered as covering the particle but rather that it is located in the vicinity of the Pb-Pd particle.

The IR results cannot be explained with a decoration model since it was the adsorption of CO on surface planes that was mainly affected by Pb addition. On the other hand, the narrowing of the XPS lines visible for each bimetallic catalyst compared with the monometallic one allows us to conclude to that an alloying effect between Pd and Pb is present in our catalysts. In addition the chemisorption measurements show a decrease of about 66% in the number of exposed Pd atoms when going from mono- to bimetallic catalysts (see Table 1). This could indicate a surface composition corresponding to a PdPb₂ alloy. According to the phase diagram (35) this alloy is stable at 573 K. As we found (Pb⁰/Pd)_{XPS} ratios much smaller than that predicted by any stable alloy, the cores of the particles are most likely to be made up of pure Pd.

The study of the Pb⁰/Pd ratios observed by XPS permits us to propose a model for the bimetallic particles. In fact considering the 0.09–0.05 and the 0.30–0.12% Pd-Pb catalysts, the nominal Pb⁰/Pd ratios are the same for both catalysts, while the Pb⁰/Pd ratios from XPS analyses differ by a factor of two whatever the reduction temperature. This suggests that the distribution of Pb is not the same for both catalysts. In addition, if the surface composition is the same as shown by the chemisorption results, the Pb concentration gradient from the surface to the bulk must be different for interactive and noninteractive particles. Based on the above argument we propose the model shown in Fig. 6.

We have shown (11) that the monometallic precursors, 0.09 and 0.30% Pd, were made up of particles with strong and weak interactions with the support, respectively, leading to a 1-eV difference in the binding energy of the Pd core levels by XPS analysis; moreover, these particles were modeled as flat particles with different diameters but similar

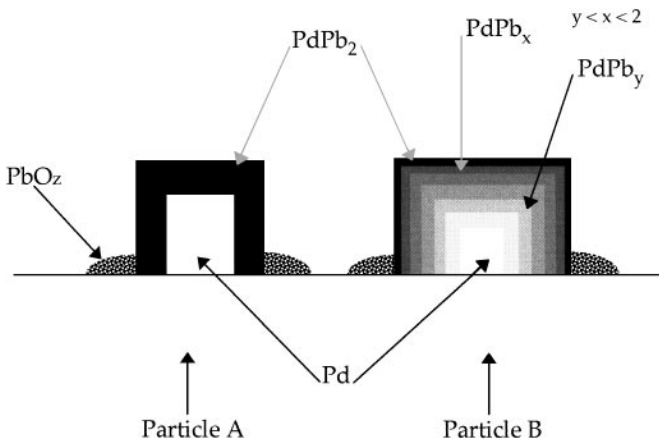


FIG. 6. Model of Pd-Pb bimetallic particles: particle A, strong interactions with the support; particle B, weak interactions with the support. Particles A and B have same height and different diameters.

heights. We have also seen that the electronic effects due to the presence of the Pd-support interactions are kept in the bimetallic catalysts; this is an indication that the interface between metal and support is made up of Pd atoms, as in the monometallic particles. One can assume that the alloy composition gradient is influenced by the interaction of the metal particle with the support impeding the penetration of lead into the bulk of these particles.

CONCLUSION

Taking into account all the results presented above it is possible to construct a model describing the Pd-Pb interaction in Pd-Pb/ α -Al₂O₃ catalysts (Fig. 6). The characterization by H₂ chemisorption, and FTIR indicates that Pd particles are partially covered by Pb. By considering γ , α , and BE modifications as well as Auger lineshape changes when comparing mono- and bimetallic samples, a modification of the Pd valence band by addition of lead is deduced. Pb XPS spectra show a mixture of Pb and lead oxide in different proportions depending on the concentration of the metals and reduction temperature. Pb forms an alloy with Pd and lead oxide is located in the vicinity of the metal particle. The concentration gradient of Pb depends on the particle-support interaction; Pd particles that exhibit a strong interaction have limited Pb penetration.

REFERENCES

1. Lindlar, H., *Helv. Chim. Acta* **35**, 436 (1952).
2. Burwell, R. L., "Survey of Progress in Chemistry" (A. F. Scott, Ed.), Vol. 8. Academic Press, New York, 1977.
3. Lindlar, H., and Dubois, R., *Org. Synth.* **46**, 89 (1966).
4. Schlögl, R., Noack, K., Zbinden, H., and Reller, A., *Helv. Chim. Acta* **70**, 627 (1987).
5. Palczewska, W., Jablonski, A., Kaszkur, Z., Zuba, G., and Wernisch, J., *J. Mol. Cat.* **25**, 307 (1984).
6. Stachurski, J., and Thomas, J. M., *Catal. Lett.* **1**, 67 (1988).
7. Boitiaux, J.-P., Cosyns, J., Derrien, M., and Léger, G., *Hydrocarbon Process* **51**, (1985).
8. Aduriz, H. R., Bodnariuk, P., Coq, B., and Figueras, F., *J. Catal.* **119**, 97 (1989).
9. Lievin, D. Z., Besprozvanny, A. M., Mietamied, A., and Kiperman, S. L., *Kinet. Katal.* **12**, 1455 (1971).
10. Lievin, D. Z., Besprozvanny, A. M., Kononov, N. F., and Kucherov, W. F., *Z. Prikl. Khim.* **41**, 1551 (1968).
11. Goetz, J., Volpe, M. A., Sica, A. M., Gigola, C. E., and Touroude, R., *J. Catal.* **153**, 86 (1995).
12. Margitfalvi, J., Hegedus, M., Göbölös, S., Kern Talas, E., Szedlacek, P., Szabo, S., and Nagy, F., in "Proceedings, 8th International Congress on Catalysis, Berlin, 1984." Dechema, Frankfurt-am-Main, 1984.
13. Travers, C., Bournonville, J. P., and Martino, G., in "Proceedings, 8th International Congress on Catalysis, Berlin, 1984." Dechema, Frankfurt-am-Main, 1984.
14. Doniach, S., and Sunjic, M., *J. Phys. C* **3**, 285 (1970).
15. Shirley, D. A., *Phys. Rev. B* **5**, 4907 (1972).
16. Scofield, J. H., *J. Electron. Spectrosc. Relat. Phenom.* **8**, 129 (1976).
17. Aduriz, H. R., Gigola, C. E., Sica, A. M., Volpe, M. A., and Touroude, R., *Catal. Today* **15**, 459 (1992).
18. (a) Sheu, L. L., Karpinski, Z., and Sachtler, W. M. H., *J. Phys. Chem.* **93**, 4890 (1989). (b) Binet, C., Jadi, A., and Lavalley, J. C., *J. Chim. Phys.* **86**, 451 (1989).
19. Primet, M., Mathieu, M. V., and Sachtler, W. M. H., *J. Catal.* **44**, 324 (1976).
20. Bastein, A. G. T. M., Toolenaar, F. J. C. M., and Ponec, V., *J. Catal.* **90**, 88 (1984).
21. van Santen, R. A., *J. Chem. Soc. Faraday Trans. 1* **83**, 1915 (1987).
22. van Santen, R. A., *J. Mol. Catal.* **54**, 288 (1989).
23. Anderson, A. B., and Awad, M. K., *J. Am. Chem. Soc.* **107**, 7854 (1985).
24. Nieuwenhuys, B. E., Ponec, V., van Koeten, G., van Leeuwen, P. W. N. M., and van Santen, R. A., in "Catalysis" (J. A. Moulijn, P. W. N. M. van Leeuwen, and R. A. van Santen, Eds.), Chap. IV, Studies in Surface Science and Catalysis, Vol. 79. Elsevier, Amsterdam, 1993.
25. Wertheim, G. K., and Citrin, P. A., "Photoemission in Solids" (M. Cardona and L. Ley, Eds.), Vol. I, p. 197. Springer, Berlin, 1978.
26. van Attekum, P. M. Th., and Trooster, J. M., *J. Phys.* **9**, 2287 (1979).
27. Castellani, N., and Légaré, P., *J. Electron. Spectrosc. Relat. Phenom.* **74**, 99 (1995).
28. Hillbrecht, F. U., and Fuggle, J. C., *Phys. Rev. B* **25**, 3550 (1982).
29. Hillbrecht, F. U., and Fuggle, J. C., *Phys. Rev. B* **27**, 2179 (1983).
30. Balakrishnan, K., and Schwank, J., *J. Catal.* **127**, 287 (1991).
31. Bouwman, R., and Biloen, P., *J. Catal.* **48**, 209 (1977).
32. Biloen, P., Heller, J. N., Verbeek, H., Dautzenberg, F. M., and Sachtler, W. M. H., *J. Catal.* **63**, 112 (1980).
33. Kim, K. S., O'Leary, T. J., and Winograd, N., *Anal. Chem.* **45**, N13 (1973).
34. Wendt, G., and Meinecke, C., *Z. Chem.* **28**, 109 (1988).
35. (a) Marcotte, V. C., *Met. Trans. B* **88**, 185 (1977); (b) Ellner, M., Gödecke, T., and Schubert, K., *Z. Metallkunde* **64**, 566 (1973).